

Spin-Orbit Coupling, Antilocalization, and Parallel Magnetic Fields in Quantum Dots

D. M. Zumbuhl,¹ J. B. Miller,^{1,2} C. M. Marcus,¹ K. Campman,³ and A. C. Gossard³¹Department of Physics, Harvard University, Cambridge, Massachusetts 02138²Division of Engineering and Applied Sciences, Harvard University, Cambridge, Massachusetts 02138³Department of Electrical and Computer Engineering,
University of California, Santa Barbara, California 93106

We investigate antilocalization due to spin-orbit coupling in ballistic GaAs quantum dots. Antilocalization that is prominent in large dots is suppressed in small dots, as anticipated theoretically. Parallel magnetic fields suppress both antilocalization and also, at larger fields, weak localization, consistent with random matrix theory results once orbital coupling of the parallel field is included. In situ control of spin-orbit coupling in dots is demonstrated as a gate-controlled crossover from weak localization to antilocalization.

The combination of quantum coherence and electron spin rotation in mesoscopic systems produces a number of interesting and novel transport properties. Numerous proposals for potentially revolutionary electronic devices that use spin-orbit (SO) coupling have appeared in recent years, including gate-controlled spin rotators [1] as well as sources and detectors of spin-polarized currents [2]. It has been predicted that the effects of some types of SO coupling will be strongly suppressed in small 0D systems, i.e., quantum dots [3, 4, 5]. This suppression as well as overall control of SO coupling will be important if quantum dots are used to store electron spin states as part of a future information processing scheme.

In this Letter, we investigate SO effects in ballistic-chaotic GaAs/AlGaAs quantum dots. We identify the signature of SO coupling in ballistic quantum dots to be antilocalization (AL), leading to characteristic magnetoconductance curves, analogous to known cases of disordered 1D and 2D systems [6, 7, 8, 9, 10, 11]. AL is found to be prominent in large dots and suppressed in smaller dots, as anticipated theoretically [3, 4, 5]. Results are generally in excellent agreement with a new random matrix theory (RMT) that includes SO and Zeeman coupling [5]. Moderate magnetic fields applied in the plane of the 2D electron gas (2DEG) in which the dots are formed cause a crossover from AL to weak localization (WL). This can be understood as a result of Zeeman splitting, consistent with RMT [5]. At larger parallel fields WL is also suppressed, which is not expected within RMT. The suppression of WL is explained quantitatively by orbital coupling of the parallel field, which breaks time-reversal symmetry [12]. Finally, we demonstrate in situ electrostatic control of the SO coupling strength by tuning from AL to WL in a dot with a center gate.

It is well known that in mesoscopic samples coherent backscattering of time-reversed electron trajectories leads to a conductance minimum (WL) at $B = 0$ in the spin-invariant case, and a conductance maximum (AL) in the case of strong SO coupling [6]. In semiconductor heterostructures, SO coupling results mainly from electric fields [13] (appearing as magnetic fields in the electron frame) leading to momentum dependent spin precessions due to crystal inversion asymmetry (Dresselhaus term [14]) and heterointerface asymmetry (Rashba term [15]).

SO coupling effects have been previously measured using AL in GaAs 2DEGs [8, 9, 10] and other 2D heterostructures [11]. Other means of measuring SO coupling in heterostructures, such as from Shubnikov-de Haas oscillations [16] and Raman scattering spectroscopy [17] are also quite developed. SO effects have also been reported in mesoscopic systems (comparable in size to the phase coherence length) such as Aharonov-Bohm rings, wires, and carbon nanotubes [18]. Recently, parallel field effects of SO coupling in quantum dots were measured [19, 20]. In particular, an observed reduction of conductance fluctuations in a parallel field [20] was explained by including SO effects [4, 5], leading to an important extension of random matrix theory (RMT) to include new symmetry classes associated with SO and Zeeman coupling [5].

This RMT addresses quantum dots coupled to two reservoirs via N total conducting channels, with $N \rightarrow 1$. It assumes $(\epsilon; z) \rightarrow E_T$, where $\epsilon = N/(2\pi)$ is the level broadening due to escape, z is the mean level spacing, $z = g_B B$ is the Zeeman energy and E_T is the Thouless energy (Table I). Decoherence is included as a fictitious voltage probe [5, 21] with dimensionless dephasing rate $N\tau = \hbar/(\epsilon\tau)$, where τ is the phase coherence time. SO lengths $l_{1,2}$ along respective principal axes [110] and $[1\bar{1}0]$ are assumed (within the RMT) to be large compared to the dot dimensions $L_{1,2}$ along these axes. We define the mean SO length $l_{so} = \sqrt{\frac{1}{2}(l_1^2 + l_2^2)}$ and SO anisotropy $\alpha_{so} = \frac{l_1 - l_2}{l_{so}}$. SO coupling introduces two energy scales: $\epsilon_{so}^1 = \epsilon_{so}^2 E_T (L_1 L_2 / l_{so}^2)^2$, which represents a spin-dependent Aharonov-Bohm-like effect, and $\epsilon_k^{so} = \frac{1}{2} E_T ((L_1 - l_1)^2 + (L_2 - l_2)^2) / l_{so}^2$, providing spin flips. AL appears in the regime of strong SO coupling, $(\epsilon_{so}^1; \epsilon_k^{so}) \gg \epsilon, \tau$, where \sim is the total level broadening $\sim = (\epsilon + \hbar/\tau)$. Note that large dots reach the strong SO regime more readily (i.e., for weaker SO coupling) than small dots. Parameters α_{so} , ϵ_{so} , and ϵ_k^{so} (a dimensionless parameter characterizing trajectory areas within the dot) are extracted from fits to dot conductance as a function of perpendicular field, B_\perp . The asymmetry parameter, α_{so} , is estimated from the dependence of magnetoconductance on parallel field, B_\parallel .

The quantum dots are formed by lateral Cr-Au de-

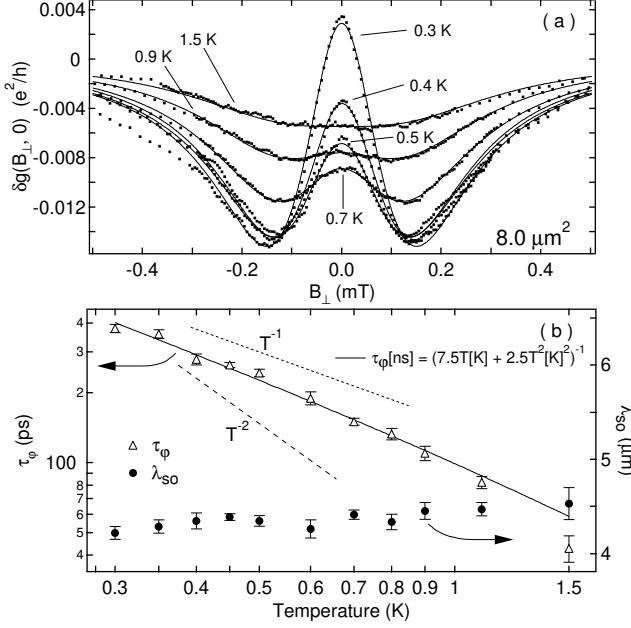


FIG. 3: (a) Difference of average conductance from its value at large B_{\perp} , $g(B_{\perp}; 0)$, for various temperatures with $B_k = 0$ for the 8.0 m^2 dot (squares), along with RMT fits (solid curves). (b) Spin-orbit lengths λ_{SO} (circles) and phase coherence times τ_{ϕ} (triangles) as a function of temperature, from data in (a).

agreement between experiment and the new RMT.

We next consider the influence of a parallel magnetic field on average magnetoelectroconductance. In order to apply tesla-scale B_k while maintaining subgauss control of B_{\perp} , we mount the sample with the 2DEG aligned to the axis of the primary solenoid (accurate to 1°) and use an independent split-coil magnet attached to the cryostat to provide B_{\perp} as well as to compensate for sample misalignment [20]. Figure 2 shows plots of the deviation of the shape-averaged conductance from its value at B_{\perp}

$g_0 = A$ (i.e., with time-reversal symmetry fully broken by B_{\perp}), $g(B_{\perp}; B_k) = \langle g(B_{\perp}; B_k) \rangle - \langle g(B_{\perp}; 0 = A; B_k) \rangle$. Figure 2(a) shows $g(B_{\perp}; B_k)$ as a function of B_{\perp} at several values of B_k , along with fits of RMT [5] in which parameters λ_{SO} , τ_{ϕ} , and γ have been set by a single fit to the $B_k = 0$ data. The low-field dependence of $g(0; B_k)$ on B_k (Fig. 2(b)) then allows the remaining parameter, λ_{SO} , to be estimated as described below.

Besides λ_z (which is calculated using $g = 0.44$ rather than t), parallel field combined with SO coupling introduces an additional new energy scale, $\lambda_z^{\text{SO}} = \frac{z_z^2 A}{2E_T} P$, $i, j = 1, 2$, $\frac{1}{i} \frac{1}{j}$, where λ_z is a dot-dependent constant and $\hat{l}_{i,j}$ are the components of a unit vector along B_k [5]. Because orbital effects of B_k on $g(B_{\perp}; B_k)$ dominate at large B_k , λ_z^{SO} must instead be estimated from RMT fits of $\text{var}(g)$ with already-broken time reversal symmetry, which is unaffected by orbital coupling [24].

The RMT formulation [5] is invariant under $\lambda_{\text{SO}} \rightarrow r \lambda_{\text{SO}}$, where $r = L_1/L_2$ [25], and gives an extremal value of $g(0; B_k)$ at $\lambda_{\text{SO}} = \frac{r}{1+r}$. As a consequence, fits to $g(0; B_k)$ cannot distinguish between λ_{SO} and $r \lambda_{\text{SO}}$. As

shown in Fig. 2(b), data for the 8 m^2 dot ($r \approx 2$) are consistent with $\lambda_{\text{SO}} \approx 2$ and appear best fit to the extremal value, $\lambda_{\text{SO}} \approx 1.4$. Values of λ_{SO} that differ from one indicate that both Rashba and Dresselhaus terms are significant, which is consistent with 2D data taken on the same material [10].

Using $\lambda_{\text{SO}} = 1.4$ and values of λ_{SO} , τ_{ϕ} , and γ from the $B_k = 0$ fit, RMT predictions for $g(B_{\perp}; B_k)$ agree well with experiment up to about $B_k \approx 0.2 \text{ T}$ (Fig. 2(a)), showing a crossover from AL to WL. For higher parallel fields, however, experimental g 's are suppressed relative to RMT predictions. By $B_k \approx 2 \text{ T}$, WL has vanished in all dots (Fig. 2(c)) while RMT predicts significant remaining WL at large B_k . The full range of $g(0; B_k)$ for the three dots is shown in Fig. 2(c). The center-gated (5.6 m^2) dot and the small (1.2 m^2) dot show WL for all B_k , and a similar suppression of WL above $B_k \approx 2 \text{ T}$.

One would expect WL/AL to vanish once orbital effects of B_k break time reversal symmetry. Following Ref. [12] (FJ), we account for this with a suppression factor $f_{\text{FJ}}(B_k) = (1 + \frac{1}{B_k} = \frac{1}{\text{esc}})^{-1}$, where $\frac{1}{B_k} = a B_k^2 + b B_k^6$, and assume that the combined effects of SO coupling and flux threading by B_k can be written as a product, $g(0; B_k) = g_{\text{RMT}}(0; B_k) f_{\text{FJ}}(B_k)$. The B_k^2 term reflects surface roughness or dopant inhomogeneities; the B_k^6 term reflects the asymmetry of the quantum well. We consider fits taking a as a fit parameter (a_1 , Table I) with $b = 1.4 \times 10^8 \text{ s}^1 \text{ T}^6$ fixed, obtained from self-consistent simulations [26], or allowing both a and b to be fit parameters (a_2 and b_2 , Table I). Figure 2(c) shows that allowing both to be free is only significant for the (unusually shaped) center-gated dot; for the small and large dots, the single-parameter (a) fit gives good quantitative agreement.

We next consider the effects of temperature and dephasing. We find that increased temperature reduces the overall magnitude of g and also suppresses AL compared to WL, causing AL at 300 mK to become WL by 1.5 K (maximum of $g(B_{\perp}; 0)$ at $B_{\perp} = 0$ becomes minimum) in the 8 m^2 dot (Fig. 3a). Fits of RMT to $g(B_{\perp}; 0)$ yield λ_{SO} values that are roughly independent of temperature (Fig. 3b), consistent with 2D results [9], and τ_{ϕ} values that decrease with increasing temperature. Dephasing is well described by the empirical form $(\tau_{\phi} [\text{ns}])^{-1} = 7.5 \text{ T} [\text{K}] + 2.5 (\text{T} [\text{K}])^2$, consistent with previous measurements in low-SO dots [27]. As temperature increases, long trajectories that allow large amounts of spin rotations are being cut off by the decreasing τ_{ϕ} , and the AL peak is diminished, as observed.

Finally, we demonstrate in situ control of the SO coupling using a center-gated dot. Figure 4 shows the observed crossover from AL to WL as the gate voltage V_g is tuned from $+0.2 \text{ V}$ to -1 V . At $V_g = -1 \text{ V}$, electrons beneath the center gate are fully depleted producing a dot of area 5.8 m^2 which shows WL. In the range of $V_g \approx -0.3 \text{ V}$, the region under the gate is not fully depleted and the amount of AL is controlled by modifying the density under the gate. Note that for $V_g > 0 \text{ V}$ the

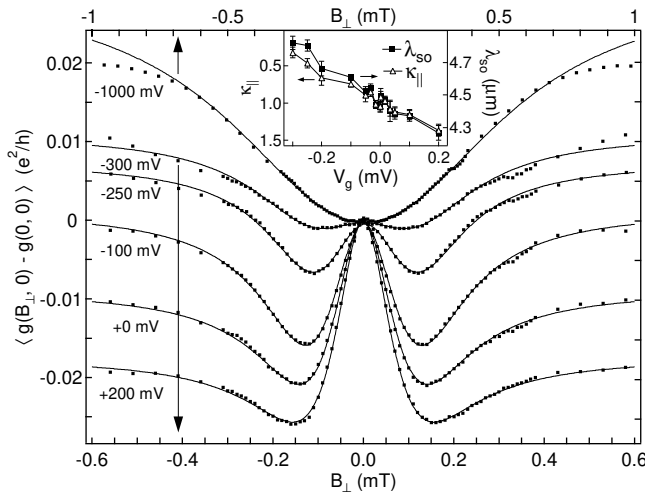


FIG. 4: Difference of average conductance $\langle g \rangle$ from its value at $B_{\perp} = 0$ as a function of B_{\perp} for various center gate voltages V_g in the center-gated dot (squares), along with fits to RMT [5]. Good fits are obtained though the theory assumes homogeneous SO coupling. Error bars are the size of the squares. Inset: λ_{so} and k_{\parallel} as a function of V_g extracted from RMT fits, see text.

AL peak is larger than in the ungated 8 nm^2 dot. We interpret this enhancement not as a removal of the SO suppression due to an inhomogeneous SO coupling [28], which would enhance AL in dots with $L = \lambda_{so} = 1$ (not

the case for the 8 nm^2 dot), but rather as the result of increased SO coupling in the higher-density region under the gate when $V_g > 0 \text{ V}$.

One may wish to use the evolution of $W L / A L$ as a function of V_g to extract SO parameters for the region under the gate. To do so, the dependence may be ascribed to either a gate-dependent λ_{so} or to a gate-dependence of a new parameter $k_{\parallel} = \frac{\lambda_{so}}{k} = ((L_1 = 1)^2 + (L_2 = 2)^2)^{-1/2} \lambda_{so}$. Both options give equally good agreement with the data (fits in Fig. 4 assume $\lambda_{so}(V_g)$), including the parallel field dependence (not shown). Resulting values for λ_{so} or k_{\parallel} (assuming the other fixed) are shown in the inset in Fig. 4. We note that the 2D samples from the same wafer did not show gate-voltage dependent SO parameters [10]. However, in the 2D case a cubic Dresselhaus term that is not included in the RMT of Ref. [5] was significant. For this reason, fits using [5] might show $\lambda_{so}(V_g)$ though the 2D case did not. Further investigation of the gate dependence of SO coupling in dots will be the subject of future work.

We thank I. A. Leiner, B. A. Ithaler, P. Brouwer, J. Cremer, V. Falko, J. Folk, B. Halperin, T. Jungwirth and Y. Lyanda-Geller. This work was supported in part by DARPA-QuIST, DARPA-SpinS, ARO-MURI and NSF-NSEC. Work at UCSB was supported by QUEST, an NSF Science and Technology Center. JBM acknowledges partial support from NDSEG.

- [1] S. Datta and B. Das, Appl. Phys. Lett. 56, 665 (1990).
- [2] E. N. Bulgakov et al., Phys. Rev. Lett. 83, 376 (1999); A. A. Kiselev and K. W. Kin, Appl. Phys. Lett. 78, 775 (2001); S. K. Eppeler and R. Winkler, Phys. Rev. Lett. 88, 46401 (2002).
- [3] A. V. Khaetskii and Y. V. Nazarov, Phys. Rev. B 61, 12639 (2000); A. V. Khaetskii and Y. V. Nazarov, Phys. Rev. B 64, 125316 (2001).
- [4] B. I. Halperin et al., Phys. Rev. Lett. 86, 2106 (2001).
- [5] I. L. A. Leiner and V. I. Fal'ko, Phys. Rev. Lett. 87, 256801 (2001); J. N. H. J. Cremer, P. W. Brouwer, B. I. Halperin, I. L. A. Leiner and V. I. Fal'ko, (to be published).
- [6] S. Hikami et al., Prog. Theor. Phys. 63, 707 (1980); B. L. Altshuler et al., Sov. Phys. JETP 54, 411 (1981).
- [7] G. Bergmann, Phys. Rep. 107, 1 (1984).
- [8] P. D. Dresselhaus et al., Phys. Rev. Lett. 68, 106 (1992).
- [9] O. M. Ilb et al., Phys. Rev. Lett. 65, 1494 (1990).
- [10] J. B. Miller, D. M. Zumbuhl, C. M. Marcus, Y. B. Lyanda-Geller, K. Campman, and A. C. Gossard, cond-mat/0206375.
- [11] W. Knapp et al., Phys. Rev. B 53, 3912 (1996).
- [12] V. I. Fal'ko and T. Jungwirth, Phys. Rev. B 65, 81306 (2002); J. S. Meyer et al., cond-mat/0105623 (2001).
- [13] M. I. Dyakonov and V. I. Perel', Sov. Phys. JETP 33, 1053 (1971).
- [14] G. Dresselhaus, Phys. Rev. 100, 580 (1955).
- [15] Y. L. Bychkov, E. I. Rashba, J. Phys. C 17, 6093 (1983).
- [16] J. P. Heida et al., Phys. Rev. B 57, 11911 (1988); S. J. Papadakis et al., Science 283, 2056 (1999); D. G. Rundler, Phys. Rev. Lett. 84, 6074 (2000).
- [17] B. Jusserand et al., Phys. Rev. B 51, 4707 (1995).
- [18] C. Kurdak et al., Phys. Rev. B 46, 6846 (1992); A. G. Aronov and Y. B. Lyanda-Geller, Phys. Rev. Lett. 70, 343 (1993); A. F. Morpurgo et al., Phys. Rev. Lett. 80, 1050 (1998); J. Nitta et al., Appl. Phys. Lett. 75, 695 (1999); H. R. Shea et al., Phys. Rev. Lett. 84, 4441 (2000); H. A. Engeland D. Loss, Phys. Rev. B 62, 10238 (2000); A. Braggio et al., Phys. Rev. Lett. 87, 146802 (2001); F. M. Irelles and G. Kirczenow, Phys. Rev. B 64, 24426 (2001).
- [19] B. Hackens et al., Physica E 12, 833 (2002).
- [20] J. A. Folk et al., Phys. Rev. Lett. 86, 2102 (2001).
- [21] M. Buttiker, Phys. Rev. B 33, 3020 (1986); H. U. Baranger and P. A. Mello, Phys. Rev. B 51, 4703 (1995); P. W. Brouwer and C. W. J. Beenakker, Phys. Rev. B 55, 4695 (1997).
- [22] All measured densities are below the threshold for second subband occupation $n \approx 6 \times 10^{15} \text{ m}^{-2}$, which is known from Shubnikov-de Haas measurements and a decreasing mobility with increasing density near the threshold.
- [23] I. H. Chan et al., Phys. Rev. Lett. 74, 3876 (1995).
- [24] D. M. Zumbuhl et al., (to be published).
- [25] The symmetry is precise if one takes $\frac{z}{\lambda_{so}} = \frac{z}{2E_F} \frac{A}{\lambda_{so}}$. See Ref. [5].
- [26] V. Falko, T. Jungwirth, private communication.
- [27] A. G. Huibers et al., Phys. Rev. Lett. 81, 200 (1998); A. G. Huibers et al., Phys. Rev. Lett. 83, 5090 (1999).
- [28] P. W. Brouwer et al., Phys. Rev. B 65, 81302 (2002).